

10-22-2009

Biomechanical Model of Transhumeral Prostheses

Rebekah Freilich
University of South Florida

Follow this and additional works at: <https://digitalcommons.usf.edu/etd>



Part of the [American Studies Commons](#)

Scholar Commons Citation

Freilich, Rebekah, "Biomechanical Model of Transhumeral Prostheses" (2009). *USF Tampa Graduate Theses and Dissertations*.
<https://digitalcommons.usf.edu/etd/1972>

This Thesis is brought to you for free and open access by the USF Graduate Theses and Dissertations at Digital Commons @ University of South Florida. It has been accepted for inclusion in USF Tampa Graduate Theses and Dissertations by an authorized administrator of Digital Commons @ University of South Florida. For more information, please contact digitalcommons@usf.edu.

Biomechanical Model of Transhumeral Prostheses

by

Rebekah Freilich

A thesis submitted in partial fulfillment
of the requirements for the degree of
Master of Science in Biomedical Engineering
Department of Chemical & Biomedical Engineering
College of Engineering
University of South Florida

Major Professor: Rajiv Dubey, Ph.D.
William E. Lee, III, Ph.D.
Stephanie L. Carey, Ph.D.
M. Jason Highsmith, DPT

Date of Approval:
October 22, 2009

Keywords: Socket-Residual Limb Interface, Motion Analysis, Validation,
Reliability

©Copyright 2009, Rebekah Freilich

DEDICATION

I would like to dedicate this thesis to my family who never gave up on me.

Love you all lots.

ACKNOWLEDGMENTS

I would first like to thank everyone on my committee for all of their help and support through the entire process of completing my thesis. I could not have finished without their willingness to help. Secondly I would like to thank Greg Bauer and his team at West Coast Brace and Limb for creating the residual limb used for testing.

TABLE OF CONTENTS

LIST OF TABLES	iii
LIST OF FIGURES	iv
ABSTRACT	vi
CHAPTER 1-INTRODUCTION	1
Problem Statement	1
Importance of Socket-Residual Limb (S-RL) Interface	2
Evolution of Socket Design	5
Motion Analysis as a Tool to Measure Motion	6
Goals of the Thesis	8
Hypothesis	8
CHAPTER 2-MATERIALS AND METHODS	9
Testing Protocol	9
Experimental Design	11
Reliability and Validity	11
Data Processing	12
Marker Set	12
Segments	15
Angle Measurements and Calculations	18
Displacement	23
CHAPTER 3-RESULTS	25
Elbow Angle	25
Inferior Displacement	27
Medial/Lateral Tilt	29
Axial Rotation	30
Shoulder Angle Verification	31
CHAPTER 4-DISCUSSIONS, LIMITATIONS AND RECOMMENDATIONS FOR FUTURE WORK	32
REFERENCES	35

APPENDICES	37
Appendix A : Marker File	38
Appendix B : Vicon BodyBuilder Program for Rig	42
Appendix C: Vicon BodyBuilder Program	47

LIST OF TABLES

Table 1	Marker set used by Carey et al. [15] which also represents a typical marker set based on anatomical landmarks	7
Table 2	Data from a single trial of elbow angle calculations	19
Table 3	Example of data and statistical calculations for inferior displacement from a single trial	24
Table 4	Data from all of the elbow angle calculations	25
Table 5	Data from all of the inferior displacement trials	27
Table 6	Data from all of the tilt trials	29

LIST OF FIGURES

Figure 1	Custom Testing Apparatus	9
Figure 2	Marker set for residual limb and prosthetic socket	12
Figure 3	Marker placement on front of body	14
Figure 4	Marker placement on back of body	14
Figure 5	The 3 segments representing arm and prosthesis	15
Figure 6	Coordinate system that defines the residual limb segment	16
Figure 7	Coordinate system that defines the socket segment	17
Figure 8	Position of the goniometer on the prosthesis while measuring elbow angles	18
Figure 9	Graph of elbow component angles from a single trial	19
Figure 10	Set-up for axial rotation and tilt trials	20
Figure 11	Marks on the residual limb to measure inferior displacement of the socket on the residual limb	23
Figure 12	The inferior translation is equal to the change of position of the FSckt marker	24
Figure 13	Regression Analysis between the accepted angle values and the VICON calculated angles	26
Figure 14	Regression Analysis between the accepted displacement values and the VICON calculated distances	28
Figure 15	Regression Analysis between the accepted tilt angle and the VICON calculated distances	29
Figure 16	Regression Analysis between the accepted axial rotation angle and the VICON calculated distances	30
Figure 17	Comparison between the validated marker set and the experimental marker set during shoulder flexion	31

Figure 18 Comparison between the validated marker set and the
experimental marker set during shoulder abduction

31

BIOMECHANICAL MODEL OF TRANSHUMERAL PROSTHESES

Rebekah Freilich

ABSTRACT

It has been shown that the interface between the prosthetic socket and residual limb (S-RL) interface is an important factor in determining acceptance and outcomes of upper limb prostheses. [1] Among the most common complaint from amputees is that the prosthesis is uncomfortable due to developing skin irritation which is usually attributed to poor fit (Nielson 1990). In order to understand why skin irritations can and do occur it is imperative to examine the biomechanical properties of the S-RL interface. A primary reason behind the development of skin irritation is instability of the socket upon the residuum. Alley (2009) asserts that excess slip, axial rotation, and translation are the facets of instability that cause skin irritations due to friction and shear. Measuring the motion at the S-RL interface is not commonly done and therefore there is still no valid and reliable method to quantify the motion clinically.

A licensed prosthesis fabricated a transhumeral residual limb model to fit within a typical, harness suspended transhumeral prosthesis. A custom testing apparatus was built to hold the residual limb model and prosthesis for testing.

Eight infrared markers were placed on the prosthesis and residual limb model: Two each respectively on the “wrist”, elbow axis, socket, and on the residual limb model. The model consists of 3 rigid segments, the forearm, socket, and residual limb.

Pearson r correlations were done to see how strongly correlated the motion analysis calculated values were to the accepted values. All results were significant with a $r \leq .95$ and $p < .05$.

CHAPTER 1-INTRODUCTION

Problem Statement

Technological advancements in upper limb prosthetics have lead to improved prosthetic function and design. However, currently the ability to quantify the motion of particularly upper limb prosthetics is lagging. The marker sets for the upper body are based on anatomical landmarks which may or may not be present depending on the location of the amputation.

Another problem basing the marker sets on anatomical landmarks is that the residual limb and socket are grouped together as one segment. By grouping the prosthetic socket and residual limb together one is assuming that the long axis of the socket and residual limb are always aligned, which would not be the case if there was any medial/lateral tilt in the frontal plane of the socket on the residual limb. Despite the fact that the motion at interface between the residual limb and socket has become an important discussion topic there is currently no valid and reliable way to quasi-statically measure the motion at the interface.

Importance of Socket-Residual Limb (S-RL) Interface

It has been shown that the interface between the prosthetic socket and residual limb (S-RL) interface is an important factor in determining acceptance and outcomes of upper limb prostheses. [1] Among the most common complaint from amputees is that the prosthesis is uncomfortable due to developing skin irritation which is usually attributed to poor fit .[2] In order to understand why skin irritations can and do occur it is imperative to examine the biomechanical properties of the S-RL interface. A primary reason behind the development of skin irritation is instability of the socket upon the residuum.

The skin irritations occur due to the biomechanical properties at the S-RL interface. These properties include the load distribution, transmission of forces from the user to the prosthesis, and the stability of device. These properties rely on proper fit of the socket as well as have an effect on the positional control of the prosthetic device.

Load distribution and transmission has been an important topic in both upper and lower limb prosthetics. The main principles of the current load-distribution models are the same when it comes to load bearing for both upper and lower limb: uniform distribution of load around the residual limb and concentration of load on load-tolerant parts of the limb. Alley [3] presents both the current model described above as well as his model, known as the “high-fidelity” or “compression-stabilization” model. The main difference between his

model and the current model is his involves more skeletal control through targeted soft tissue relief. [3]

Transmission of the forces from the user to the prosthetic device via the interface is also very important. In lower limb prostheses, it is particularly important because the soft tissues in the residual limb are not well suited for bearing the load of the body weight and inertial forces. [4] The S-RL interface's ability to transmit these forces greatly affects the volitional control of the prosthesis. In many current socket models there is a delay between the movement of the residual and the socket caused "by the time it takes for the soft tissue between the bone and the socket to compress to the point of realizing interface response of sufficient magnitude to effect movement." [3]

A properly designed socket will not only allow for efficient transmission of the forces from the user to the prosthesis but also optimize stability. This means that the socket will not exceed the movement needed for mobility on the residual limb, which has yet to be defined. Stability has 3 main facets: slip, axial rotation, and translation.

Slip refers to the intrinsic movement of the soft tissue to overcome the frictional force at the S-RL interface. When discussing creating new sockets it is important to talk about all of the different properties of the tissue and not just slip.

Sensinger J and Weir F [5] looked at the rotational stiffness of the S-RL interface and how much it can be modulated by the user by co-contracting their muscles. They looked at how variables such as socket length, co-contraction levels, residual limb diameter, and bone diameter affected the affected the

rotational stiffness of the S-RL interface.[5] They found that the rotational stiffness of the S-RL interface can vary over a wide range of values and that the floor and ceiling of this range depended significantly on socket length and co-contraction levels. They suggested that a distal window cut in the socket could possibly decrease the discomfort without affecting the user's ability to create torque in cases with a high rotational stiffness such as requiring a long socket. [5]The challenge is not only to attempt to decrease the discomfort caused by the rotational stiffness of the S-RL interface but also to limit the amount of slip without impinging on the range of motion the prosthetic device allows.

Rotation around the soft tissue or the long axis of the primary bone is referred to as axial rotation. Just like with slip a properly designed socket should limit the amount of axial rotation that occurs but there is no data on how much axial rotation is to be accepted. Traditional transhumeral sockets rely on auxiliary straps to control the axial rotation which subjects patients to excessive harness pressure in the axilla. [3]

Any other movement of the socket on the residual limb relative to the skeletal structure of the limb is referred to as interface translation. A lot of translation is occurs through soft tissue compression and often involves friction and shear. [3] Not only can translation lead to skin irritation but it can also complicate the control of the device. Some of the newer sockets are being designed to help minimize the slip, translation, and axial rotation at the S-RL interface. [3, 5-9]

Evolution of Socket Design

It was not until the 20th century that upper limb socket design entered the literature. In the 60's and 70's the sockets were characterized as by a reduction in the lateral trim line which caused greater stability and mobility. This was followed by an aggressive modification into the deltopectoral groove and a flattened region posteriorly just inferior to the spine of the scapula providing greater rotation control and enhanced range of motion. [8] Slowly as the 20th century ended more presentations focused on anatomical socket design.

Anatomical socket design is more than just simply matching the volume and surface shape of the residual limb. When it comes to amputations above the elbow there is a lot more unstable tissue that needs to be contained and supported than bone. However, it is still important to attempt to grab the bony structure to allow for greater stability and control.[6] This is where art and science take place in creating a socket.

Motion Analysis as a Tool to Measure Motion

Despite the interest in upper extremity motion, the analysis of the motion is still considered to be at an early stage. [10, 11] Since the 1990's there has been a large increase of the number of studies using motion analysis to measure the motion of the upper extremities. [10] The VICON Motion Analysis System is used by a number of medical and biomedical industries for capturing and measuring motion. [12]

Motion analysis was first use to measure motion in non-impaired persons. Small et.al. [13] showed that a 3D optoelectronic motion analysis is as accurate as stereoradiographic analysis of bone segments. Lowe [14] used motion analysis to validate the accuracy of observational estimates of shoulder and elbow posture .

Motion analysis has also been used to measure upper limb motion in individuals with prostheses. Most of these studies have looked at task completion with either an actual prosthesis or a simulated prosthesis. [15-17] Highsmith et al. [18] looked at different terminal devices designed to kayak. In their study they used the same marker set as Carey et al. [15] shown below in Table 1. However, the elbow calculated by the motion analysis was off by ± 10 degrees. This was one of the main reasons the experimental marker system is not based on landmarks.

Table 1 Marker set used by Carey et al. [15] which also represents a typical marker set based on anatomical landmarks

Bony landmarks used for marker placement
Marker placement
Xiphoid process of the sternum (STRN)
Middle of right scapula (RBAK) – asymmetrical marker used for digitizing
<i>Upper limbs</i>
Right acromio-clavicular joint (RSHO)
Right upper arm between the elbow and shoulder markers (RUPA)
Right lateral epicondyle approximating elbow joint axis (RELB)
Right medial epicondyle approximating elbow joint axis (RELBM) – for static trial only
Left acromio-clavicular joint (LSHO)
Left upper arm between the elbow and shoulder markers (LUPA)
Left lateral epicondyle approximating elbow joint axis (LELB)
Left medial epicondyle approximating elbow joint axis (LELBM) – for static trial only
<i>Forearms</i>
Right wrist radial side (RWRA)
Right wrist ulnar side on the pisiform (RWRB)
Dorsum of the right hand below head of 3rd metacarpal (RFIN)
Left wrist radial side (LWRA)
Left wrist ulnar side on the pisiform (LWRB)
Dorsum of the left hand below head of 3rd metacarpal (LFIN)

Goals of the Thesis

The two main goals of the thesis are:

- 1) Create a valid and reliable biomechanical model that can measure the movement at the S-RL interface.
- 2) Create a valid and reliable biomechanical model that can correctly measure the kinetics of transhumeral prostheses on a rigid body residual limb model in a laboratory setting.

Hypothesis

- 1) The measurements calculated via motion analysis in the laboratory on the rigid residual model will have a strong positive correlation ($r > .95$ $p < .05$) to the measurements of already shown to be reliable and valid tools to measure motion (Validity).
- 2) The measurements calculated for a certain construct by the motion analysis in the laboratory on the rigid residual model will not significantly differ from each other. The standard deviations of each angle and distance will be looked at as well as graphical representations of each (Reliability).

CHAPTER 2-MATERIALS AND METHODS

Testing Protocol

A licensed prosthetist fabricated a transhumeral residual limb model to fit within a typical, harness suspended transhumeral prosthesis. A custom testing apparatus was built to hold the residual limb model and prosthesis for testing.

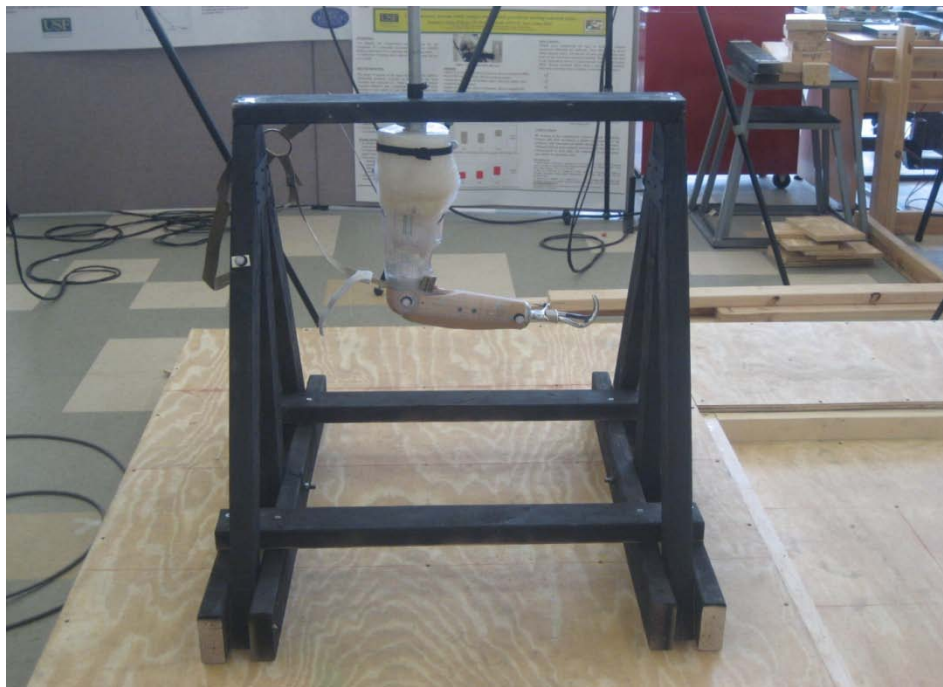


Figure 1 Custom Testing Apparatus

For the axial rotation and medial/lateral tilt testing a different residual limb was created out of plaster for easier measuring of the rotation and maneuvering. The residual limb created by the licensed prothesist has a lip on the back that would not exist on a residual limb, which does not allow for any axial rotation of the socket on the residual limb.

Experimental Design

Reliability and Validity

The main goal of this study, as mentioned above, are to create a valid and reliable marker set to measure the motion of the prosthetic arm including the motion at the S-RL interface. Reliability is the consistency of the measurements. In order for the experimental marker set to be considered reliable the standard deviation (SD) of each of the particular measurements must be less than the error of the accepted measuring device. Validity is the degree to which the measurements are measuring what they are supposed to be. In order for the experimental marker set to be considered valid a strong positive correlation ($r \geq .95$ $p < .05$) must exist between the VICON calculated measurements and the actual measurements. In Equation 1 the X refers to the actual measurements and the Y refers to the VICON calculated measurements.

$$r = \frac{\sum_{i=1}^n (X_i)(Y_i)}{\sqrt{\sum_{i=1}^n (X_i)^2 \sum_{i=1}^n (Y_i)^2}}$$

Equation 1 Pearson's r correlation

Data Processing

Marker Set

The marker set for the residual limb and prosthesis consists of 8 infrared markers: two each respectively on the “wrist” component, elbow axis, socket of prosthesis, and on the residual limb model. One marker to simulate the shoulder joint center (not shown in figure below) was added to define the axis direction for the residual limb segment. The torso and shoulder markers are consistent with those shown in table 1. The marker file for VICON can be seen in Appendix A.

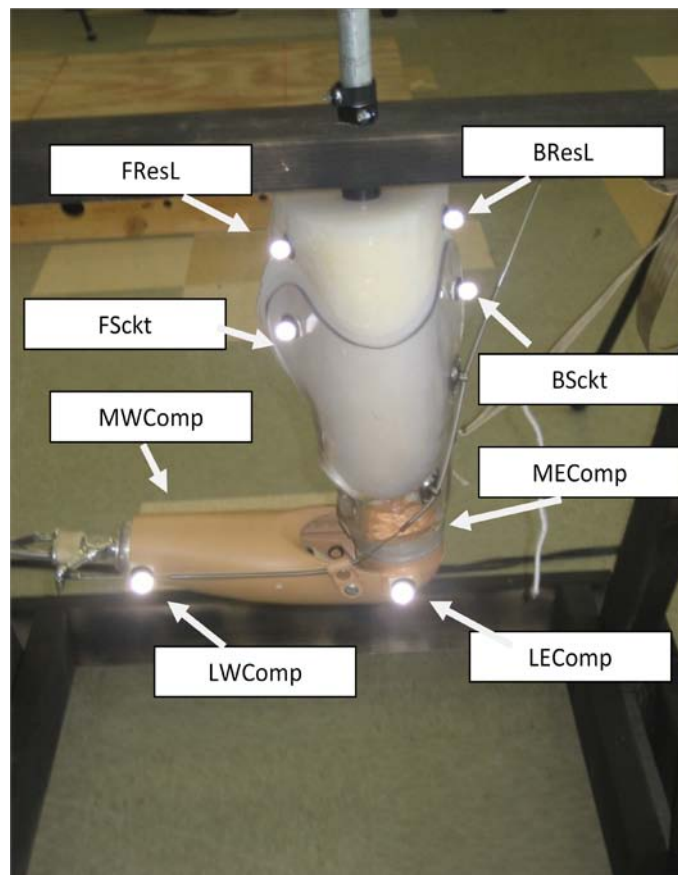


Figure 2 Marker set for residual limb and prosthetic socket

The front and back residual limb markers, FResL and BResL respectively, are located on the residual limb right above the prosthetic socket. Below them on the socket are the front and back socket markers, FSckt and BSckt respectively. On the elbow component of the prosthesis there is a marker on the medial and lateral sides of the elbow on the axis of rotation, MEComp, and LEComp respectively. The markers for the wrist component are labeled the same way as MWComp, and LWComp respectively, along the flexion / extension axis of the wrist.

The placement of the markers on the residual limb and the socket are very important to ensure that the marker set will work on all trim lines. The FResL and FSckt markers and the BResL and BSckt markers do not need to be lined up as seen in the figure but the center points between the two sets need to be lined up in all three planes.

The marker set for the torso and shoulder are consistent with those in Table 1. In the figures below the white tape represents the trim line of a prosthesis to help demonstrate the placement of the markers on the torso as well as the residual limb and prosthesis. The figures below only show the markers for the torso, residual limb, and prosthesis since the other side would be consistent with Table 1. It is imperative to note that even though the white tape and the trim line of the prosthesis used in the experiment are not the same that the ResLC and ScktC are still lined up in all three planes. As long as these two virtual points are aligned and there is a marker on the anterior and posterior parts of the residual limb and socket then the segments will be calculated correctly.

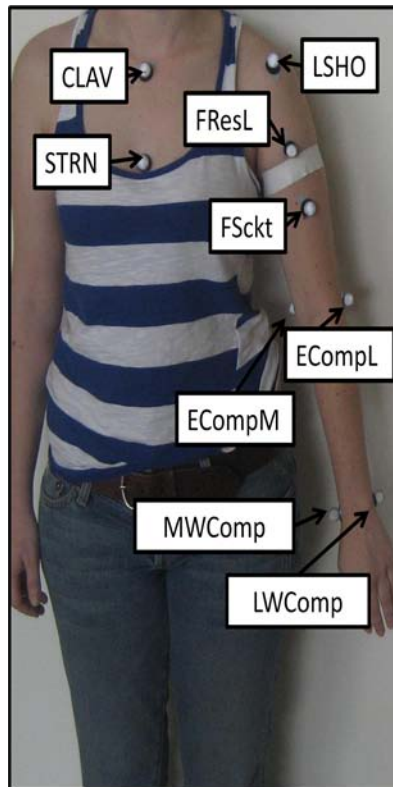


Figure 3 Marker placement on front of body

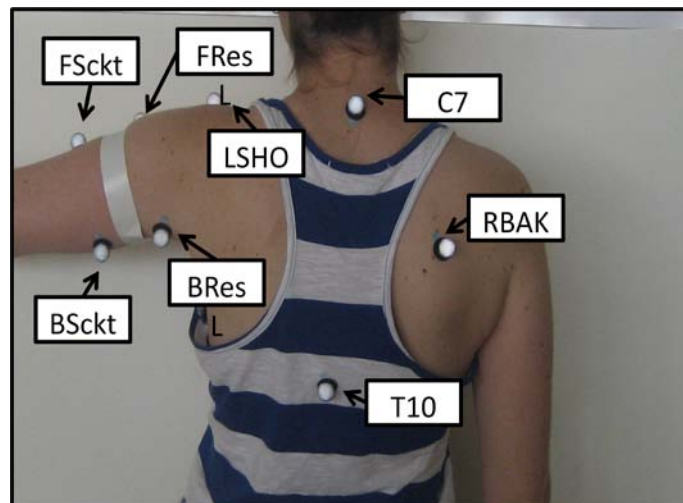


Figure 4 Marker placement on back of body

Segments

The biomechanical model of an arm with a transhumeral prosthesis is made up of 3 rigid segments: the forearm, socket, and residual limb. The main change from traditional segments is the separation of the upper arm into two segments one representing the residual limb and the other the socket. Each segment is defined by an origin and a coordinate system which are defined below.

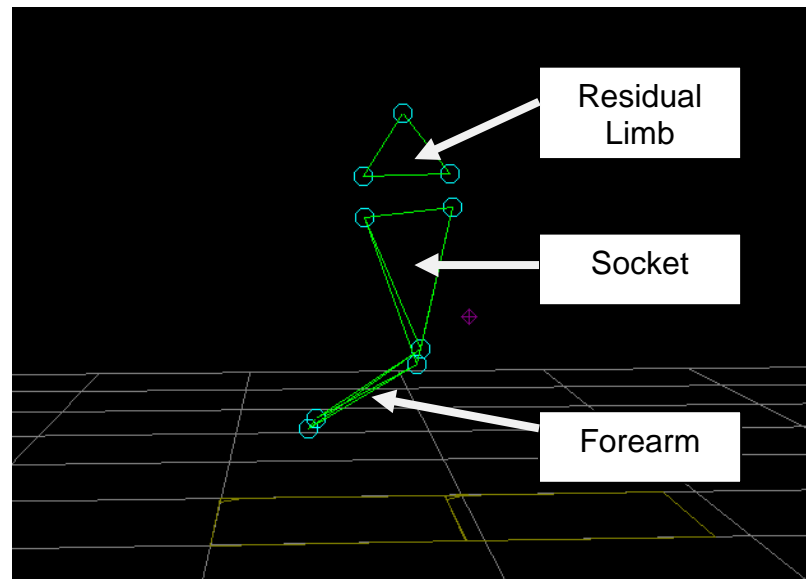


Figure 5 The 3 segments representing arm and prosthesis

The residual limb segment origin is at the ResLC which is half way between the FResL and the BResL markers. The first defining line of the segment is defined as the line from the ResLC to the shoulder joint center (SJC), which becomes the Z axis. The second defining line of the residual limb segment is from the FResL marker to the BResL marker. The Y axis, as defined by the

program, is the line perpendicular to both the first defining line and the second defining line that meets the right hand rule. Therefore using the right hand rule the Y axis would be coming out of the paper. The X axis is the line that satisfies the right hand considering the other two axes. The coordinate system for the residual limb segment is shown in Figure 6.

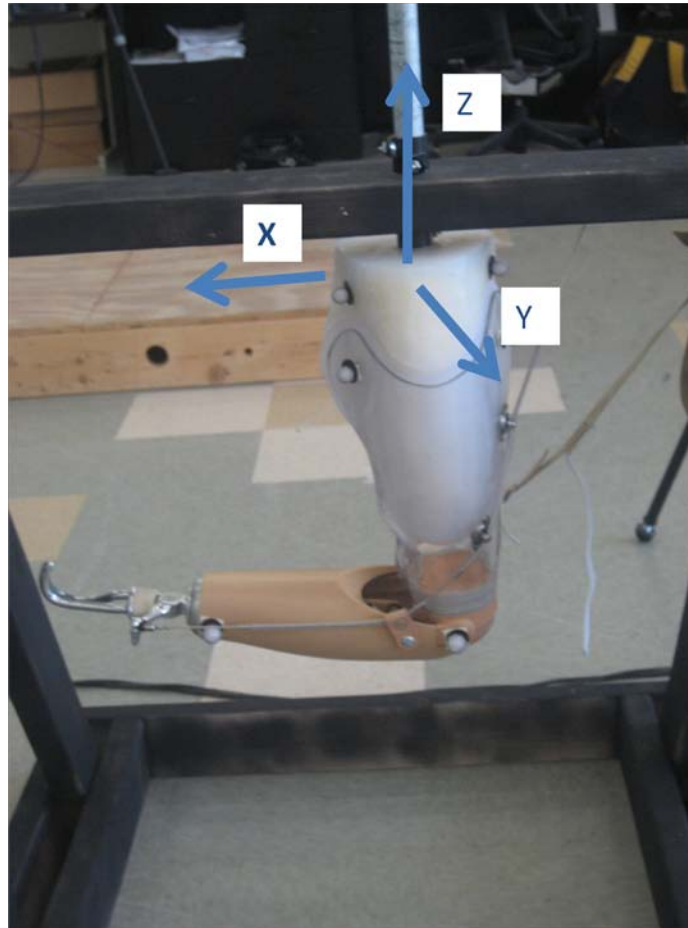


Figure 6 Coordinate system that defines the residual limb segment

The origin of the socket segment is at the elbow joint center (EcompC) which is defined as the point half way between the MEcomp and LEcomp markers. The first defining line of the socket segment is from the ECompC to the

socket center (ScktC). The second defining line of the segment is from the center of the wrist (WrstC) to the ElbwJC. Using the same definitions of each axis as described above the coordinate system for the residual segment as shown in Figure 7.

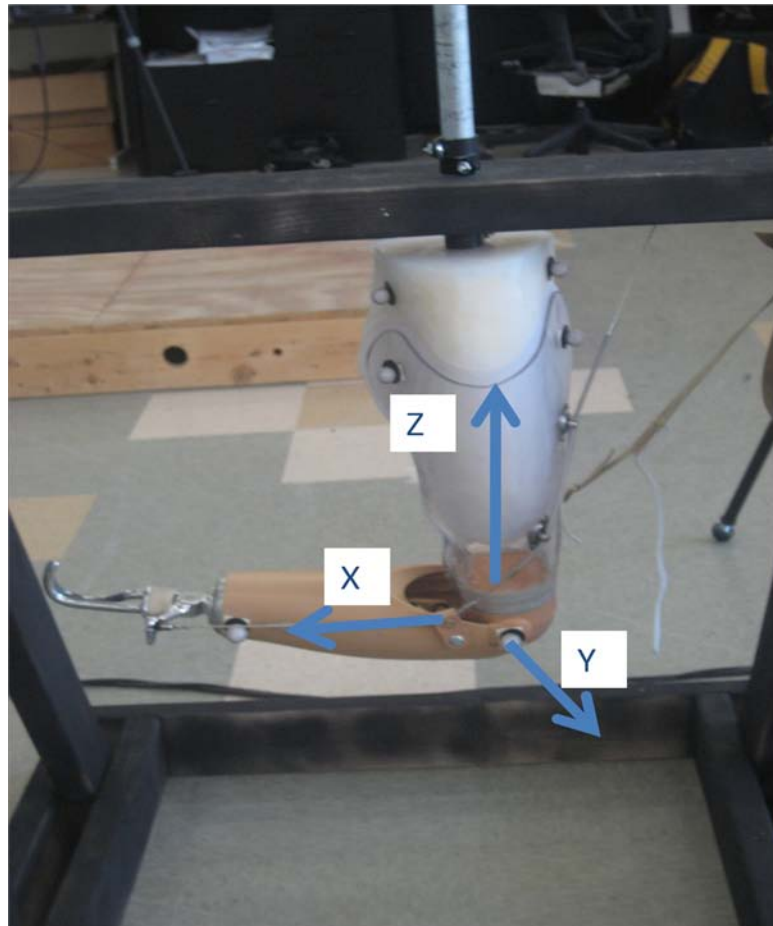


Figure 7 Coordinate system that defines the socket segment

For both the pseudo joint between the residual limb and the socket and the elbow rotation around the X, Y, and Z axis represent abduction (if possible), flexion/extension, and axial rotation respectively.

Angle Measurements and Calculations

Both quasi-static and static tests were conducted for each angle being tested. For the elbow angle a goniometer was attached to the prosthesis as shown in the figure below to determine the actual angle(s) for each test. The center of the goniometer was placed at the center of rotation of the elbow joint to ensure the most accurate measurements. The elbow was locked from 50 to 120 degrees in 10 degree increments. Quasi-static tests were also conducted from 50 to 90 degrees and then 90 to 120 degrees in 10 degree increments. The static test was conducted at each angle independently while the quasi-static test stopped at a number of angles during a single testing session.

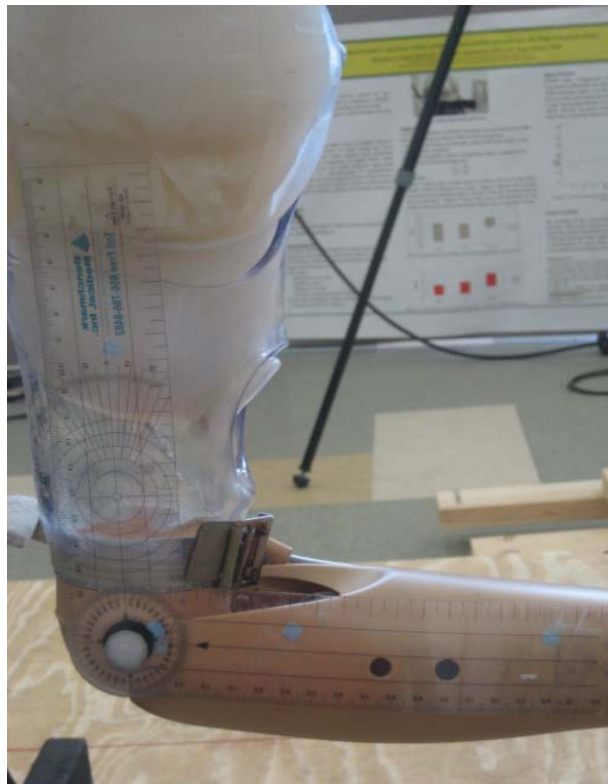


Figure 8 Position of the goniometer on the prosthesis while measuring elbow angles

Results of a single trial of elbow component angle measurements would look as follows.

Table 2 Data from a single trial of elbow angle calculations

	Goniometer (± 2)	VICON
Angle (deg)	90.0	90.9
	80.0	80.6
	70.0	70.3
	60.0	60.3
	50.0	50.5
Mean	70.0	70.5
Std. Dev.	15.8	16.0
Pearson's r	0.99995	

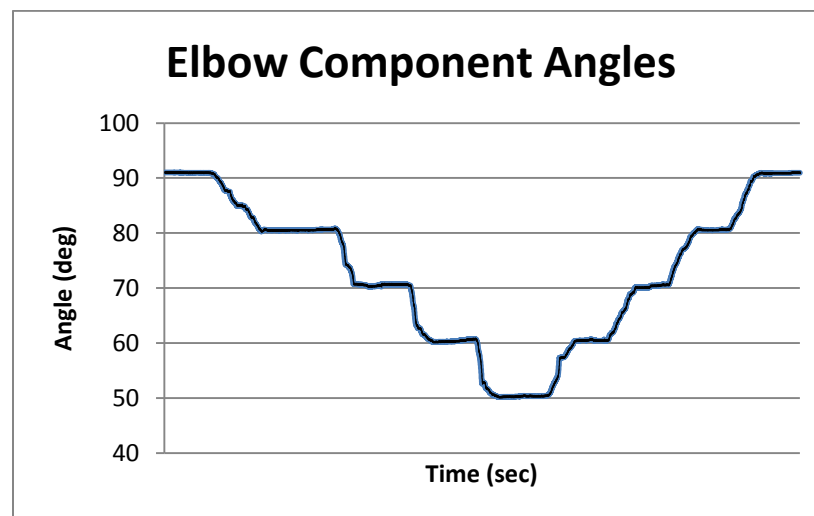


Figure 9 Graph of elbow component angles from a single trial

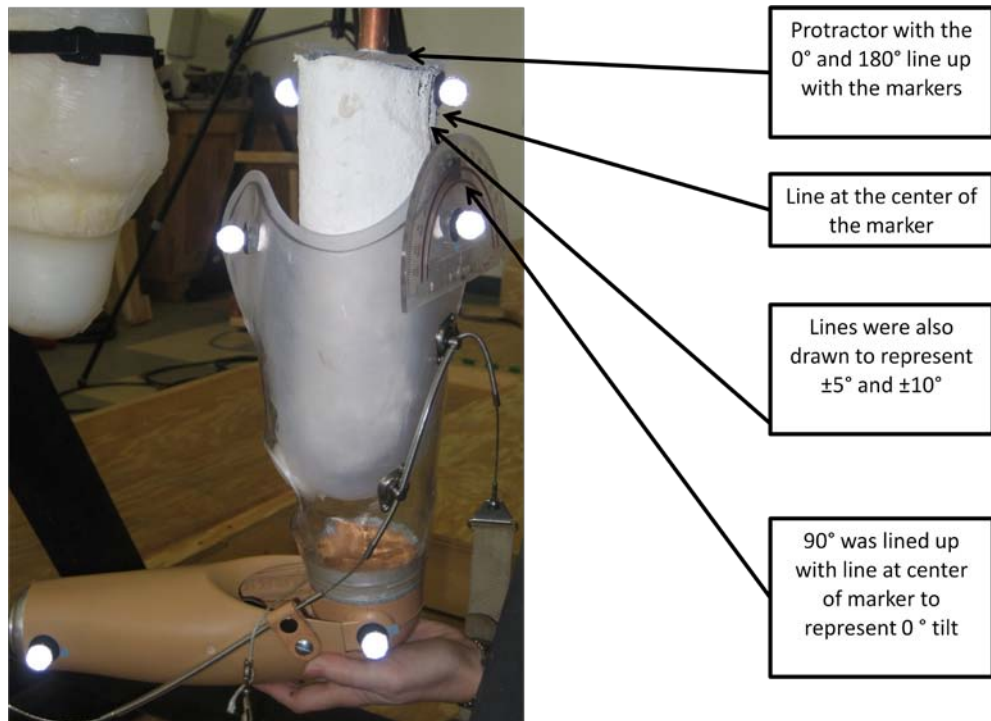


Figure 10 Set-up for axial rotation and tilt trials

For the testing of axial rotation and tilt of the prosthetic socket on the residual limb a residual limb made out of paper mache was used (shown in Figure 10). Both static and quasi-static trials were conducted for axial rotation and tilt. For axial rotation ± 5 and 10 degrees were tested and for tilt 5 and 10 degrees were measured. Each of the axial rotation and tilt trials will result in a chart link that seen in Table 2.

The shoulder angle testing was done by running trials with both the marker set described in [15] and the experimental marker set described in this

study. The calculated shoulder angles for each of the marker sets were compared graphically on the same chart. These tests ensured that the residual limb segment was moving with the prosthesis segment since the experimenter does not have a prosthesis.

BodyBuilder™ calculates angles using Euler angles. Euler angles are used to describe the rotation between two 3D coordinate systems in terms of three angles. Each of the Euler angles describes a transformation as seen in Equation 2.

$$R_x(\theta) = \begin{bmatrix} 1 & 0 & 0 \\ 0 & \cos \theta & -\sin \theta \\ 0 & \sin \theta & \cos \theta \end{bmatrix}$$

$$R_y(\theta) = \begin{bmatrix} \cos \theta & 0 & \sin \theta \\ 0 & 1 & 0 \\ -\sin \theta & 0 & \cos \theta \end{bmatrix}$$

$$R_z(\theta) = \begin{bmatrix} \cos \theta & -\sin \theta & 0 \\ \sin \theta & \cos \theta & 0 \\ 0 & 0 & 1 \end{bmatrix}$$

Equation 2 Euler angle definitions

The order of rotation of the elbow angle per the program I wrote is yxz. Euler angles describe rotation with respect to a rotating frame.[19] The rotation matrix for a yxz rotation is shown in Equation 3. The 1, 2, and 3 represent the angles of rotation around y, x, and z respectively. The transformation matrix

which is the rotational matrix times the position vector is shown in Equation 4.

The R_{11} etc in the transformation matrix correspond with that position in the rotational matrix.

$$\begin{bmatrix} c_1 c_3 - s_1 s_2 s_3 & -c_2 s_3 & c_3 s_1 + c_1 s_2 s_3 \\ c_3 s_1 s_2 + c_1 s_3 & c_2 c_3 & s_1 s_3 - c_1 c_3 s_2 \\ -c_2 s_1 & s_2 & c_1 c_2 \end{bmatrix}$$

Equation 3 Rotational matrix for elbow angle calculations

$$T = \begin{bmatrix} R_{11} & R_{12} & R_{13} & R_{11}X + R_{12}Y + R_{13}Z \\ R_{21} & R_{22} & R_{23} & R_{21}X + R_{22}Y + R_{23}Z \\ R_{31} & R_{32} & R_{33} & R_{31}X + R_{32}Y + R_{33}Z \\ 0 & 0 & 0 & 1 \end{bmatrix}$$

Equation 4 Transformation matrix for elbow angle calculations

Since the final position vector is know and the X, Y, Z are also known, the elbow angles can be calculated using inverse kinematics. All of the angles are calculated in a similar fashion with the rotational matrix being determined by the definition of the rotation in the program.

Displacement

Both static and quasi-static testing were completed for inferior displacement of the socket on the residual. Marks were placed on the residual limb in increments of .5 in from 0 to 2 inches as measured by a ruler. For the static testing the prosthesis was held at each mark independently. During the quasi-static testing the prosthesis was pulled down stopping at each mark for about 10 seconds then moving on to the next. The inferior displacement is measured by calculating the change in distance between the BResL and BSckt markers along the z axis.



Figure 11 Marks on the residual limb to measure inferior displacement of the socket on the residual limb

Results from a single trial for inferior displacement are shown below.

Table 3 Example of data and statistical calculations for inferior displacement from a single trial

	Ruler ($\pm .1$)	VICON ($\pm .02$)
Distance (in)	0.5	0.4
	1.0	0.9
	1.5	1.4
	2.0	1.9
Mean	1.3	1.2
SD	0.6	0.6
Pearson r	0.99999	

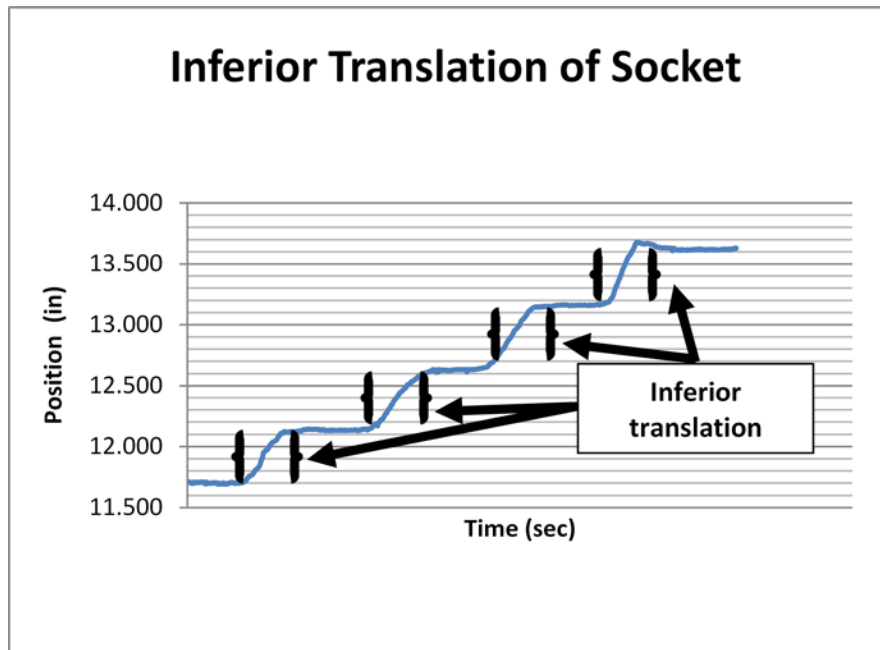


Figure 12 The inferior translation is equal to the change of position of the FSckt marker

CHAPTER 3-RESULTS

Elbow Angle

A strong positive correlation ($r = .99$ $p < .0001$) also exists between the elbow angles measured using goniometry and the elbow angles calculated by motion analysis. Since the error of the goniometer is two degrees, in order for the calculated angles from motion analysis to be reliable all of the results for a particular angle must have a difference in standard deviation less than 2 degrees.

Table 4 Data from all of the elbow angle calculations

Actual Angle (deg)	Calculated Angle (deg)											
	1	2	3	4	5	6	7	8	9	10	Mean	SD
120 ± 2	120.9	121.3	120.2	119.6	119.8	121.0	120.9	119.4	118.9	119.9	120.2	0.8
110 ± 2	111.0	110.3	109.2	110.9	109.0	111.3	109.4	111.5	109.0	110.5	110.2	1.0
100 ± 2	100.6	99.8	98.9	100.6	99.4	101.3	99.6	100.9	99.2	101.4	100.2	0.9
90 ± 2	90.9	90.7	88.8	89.3	90.7	90.8	90.9	91.4	89.5	90.3	90.3	0.8
80 ± 2	80.6	78.7	80.7	79.7	80.0	81.2	79.4	81.0	79.9	80.3	80.2	0.8
70 ± 2	70.3	69.8	68.9	70.4	69.7	72.0	69.8	71.7	70.0	70.5	70.3	0.9
60 ± 2	60.3	59.7	59.8	60.0	59.8	60.4	59.2	60.7	59.5	59.4	59.9	0.5
50 ± 2	50.5	49.7	50.2	49.9	49.5	51.0	49.0	49.4	49.0	50.9	49.9	0.7

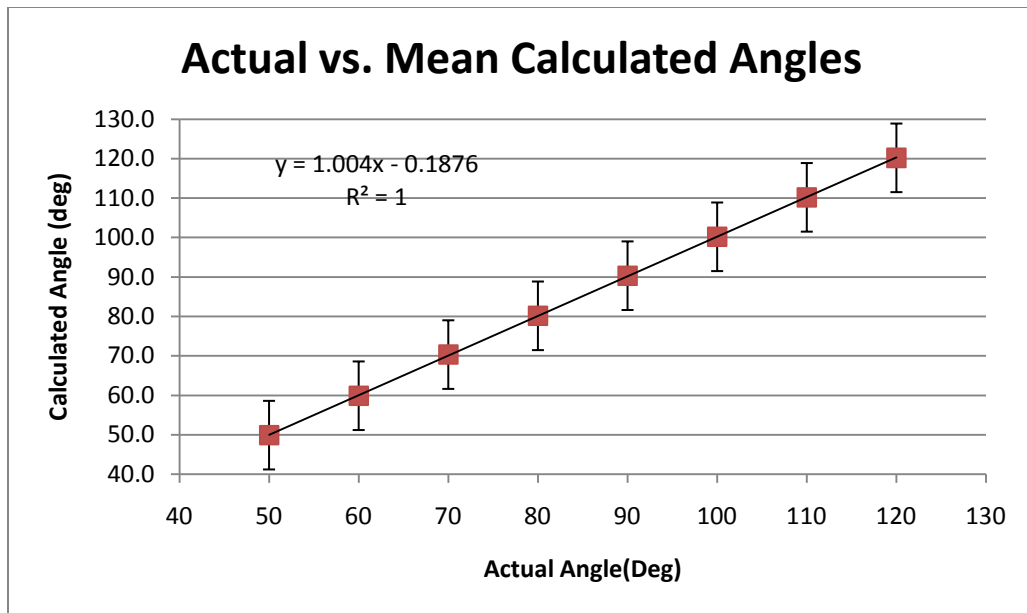


Figure 13 Regression Analysis between the accepted angle values and the VICON calculated angles. The error bars represent \pm standard error mean (SEM)

Inferior Displacement

A strong positive correlation ($r = .99$ $p \leq .0001$) also exists between the inferior displacement measured using a ruler and the distances calculated by motion analysis. Since the error of the ruler is 0.1 in, in order for the calculated distances from motion analysis to be reliable all of the results for a particular angle must have a standard deviation less than 0.1.

Table 5 Data from all of the inferior displacement trials

Actual Distance (in)	Calculated Distance ($\pm .02$)											
	1	2	3	4	5	6	7	8	9	10	Mean	SD
$0.5 \pm .1$	0.5	0.4	0.5	0.4	0.5	0.5	0.5	0.5	0.5	0.5	0.5	0.03
$1 \pm .1$	0.9	0.9	1.1	0.9	1.1	1.0	1.0	1.0	1.0	1.0	1.0	0.06
$1.5 \pm .1$	1.5	1.4	1.6	1.4	1.5	1.5	1.6	1.5	1.5	1.5	1.5	0.05
$2 \pm .1$	2.0	1.9	2.0	1.9	2.1	1.9	2.0	1.9	2.0	2.0	2.0	0.06

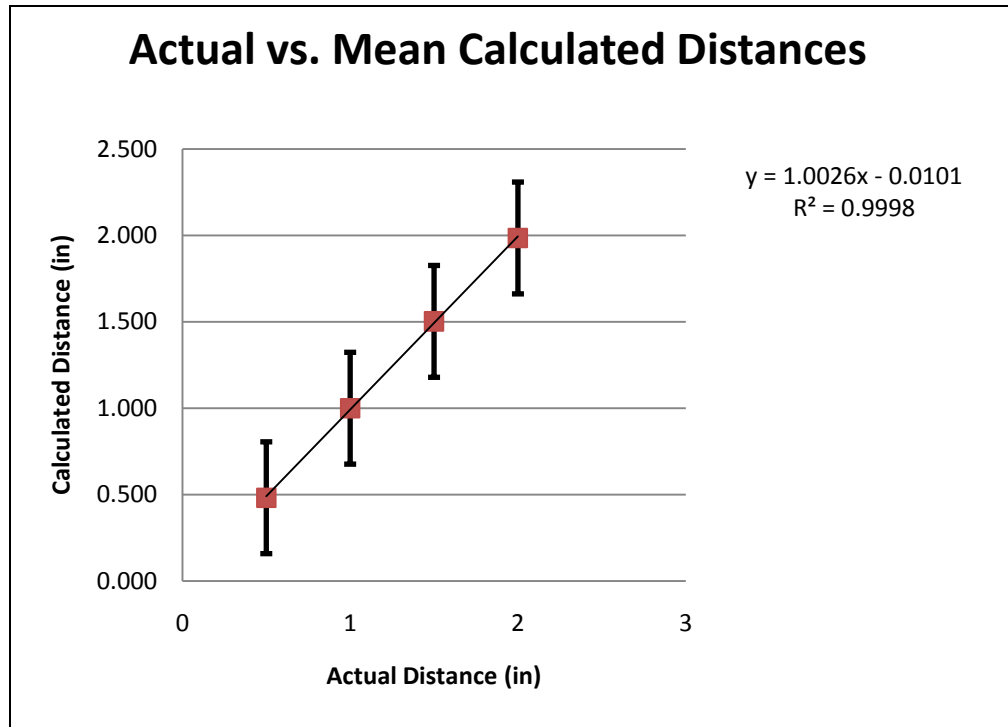


Figure 14 Regression Analysis between the accepted displacement values and the VICON calculated distances. The error bars represent \pm SEM.

Medial/Lateral Tilt

A strong positive correlation ($r = .99$ $p < .0001$) between the actual or accepted value for tilt and the VICON calculated angles for tilt of the socket on the residual limb. The error on the protractor is 1 degree therefore the difference between the two standard deviations should be less than 1 degree.

Table 6 Data from all of the tilt trials

Protractor Tilt (deg)	VICON calculated tilt (deg)											
	1	2	3	4	5	6	7	8	9	10	average	SD
5 ± 2	5.0	5.3	4.8	4.9	6.0	5.7	4.8	5.5	5.2	6.3	5.4	0.5
10 ± 2	9.5	10.0	10.6	9.4	10.4	10.2	9.7	10.3	10.3	9.9	10.0	0.4

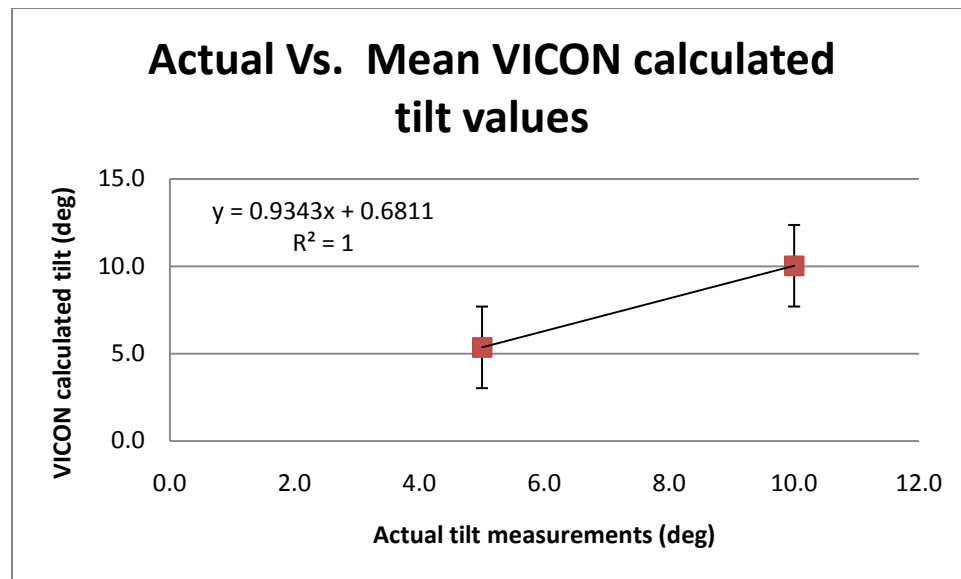


Figure 15 Regression Analysis between the accepted tilt angle and the VICON calculated distances. The error bars represent \pm SEM

Axial Rotation

A strong positive correlation ($r = .99$ $p < .0001$) between the actual or accepted value for axial rotation and the VICON calculated angles for tilt of the socket on the residual limb. The error on the protractor is 1 degree therefore the difference between the two standard deviations should be less than 1 degree.

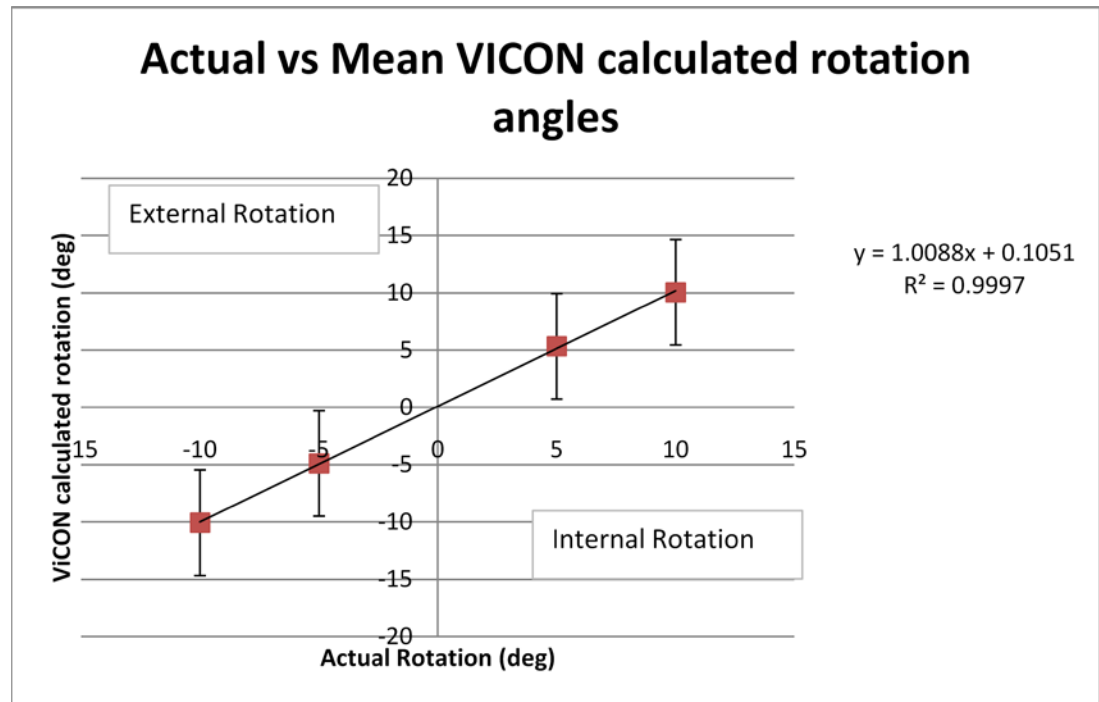


Figure 16 Regression Analysis between the accepted axial rotation angle and the VICON calculated distances. The error bars represent \pm SEM

Shoulder Angle Verification

The calculations for the shoulder angles were the same for both the validated marker set and the experimental marker set.

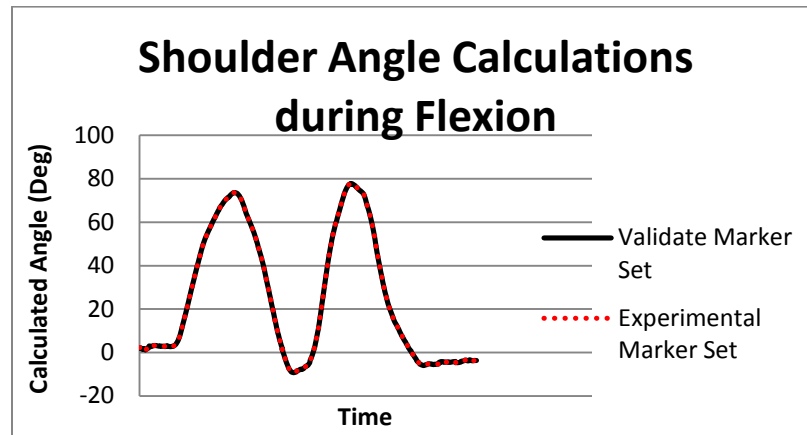


Figure 17 Comparison between the validated marker set and the experimental marker set during shoulder flexion

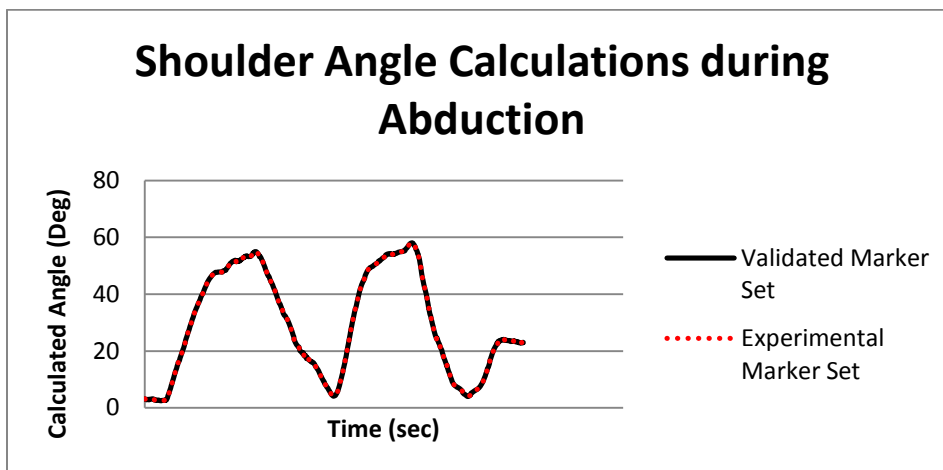


Figure 18 Comparison between the validated marker set and the experimental marker set during shoulder abduction

CHAPTER 4-DISCUSSION, LIMITATIONS AND RECOMMENDATIONS FOR FUTURE WORK

As mentioned in the introduction the analysis of upper extremity motion is still considered to be at an early stage. [10, 11] This study will add to the current research of upper extremity motion by starting the conversation about how to quantify the motion at the S-RL interface. It is imperative to keep in mind that this is just a preliminary study and limited to laboratory studies at this time.

The ability to quantify the motion at the S-RL interface will improve studies involving tranhumeral prostheses, socket design, and socket fit. The biomechanical model discussed in this paper is able to provide both valid and reliable measurements for the motion at the residual limb. Not only will this provide an objective way to quantify fit but also provide some insight as to how much motion provides the stability and control required without causing too much skin irritation that the patient chooses not to wear the prosthesis.

The most obvious limitation is the lack of any human subjects in the study. However, it is imperative to at least test the concept of the model before going through the long process of getting IRB approval and finding subjects for the test. Also due to the fact that the model was not tested on humans the experimental marker set has only been shown to be reliable and valid on a rigid body residual

model. Despite this fact this study has shown that it is possible to get valid and reliable measurements of the motion at the S-RL interface using motion analysis.

Other limitations include using only one trim line and one residual limb length. However, as mentioned above, as long as the ResLC and ScktC are still aligned the trim line will not affect the results. In terms on residual limb length, issues would arise if the residual limb was very short or if the amputation occurred at the shoulder joint. Depending on the size of the markers and the resolution of the cameras there may not be enough room to separate the residual limb and socket into two different segments. Another limitation is that I did not take into consideration properties of skin.

In order to quantify accepted values for the motion at the S-RL limb interface human subject testing needs to occur. The use of an electronic goniometer would provide an easier way to collect the accepted values of the motion rather than trying to attach both a goniometer and protractor to the individual. Also since this method is only practical in a laboratory setting it is important to try to create a tool that is more user friendly for a clinical setting. Another aspect not considered in this study is the correlation between the she forces created by the motion which is what causes the skin irritation and sores on the residual limb. In order to study the forces and pressure caused by the motion, sensors would need to be added to measure the amount of force and pressure.

The ability to measure the motion and forces at the S-RL interface is very important to the study of prosthetics. This will help researchers not only

understand how and why skin irritation can and does occur on the residual limb
but also help them determine how much motion is necessary to create the
perfect balance between control and skin irritation.

REFERENCES

1. Shultz, AE, Baade, SP, and Kuiken, TA, Expert Opinion on success factors for upper-limb prostheses. *Journal of Rehabilitation Research and Development*, 2007. 44(4): p. 8.
2. Nielson, C, Survey of amputees: functional level and life satisfaction, information needs, and the prosthetist's role. *Journal of Prosthetics and Orthotics*, 1990. 3: p. 5.
3. Alley, RD, Biomechanical Discussion of Current and Emergent Upper-Limb Prosthetic Interface Design. *The Academy Today*, 2009(June): p. 6.
4. Jia, X, Zhang, M, and Lee, WC, Load transfer mechanics between trans-tibial prosthetic socket and residual limb--dynamic effects. *J Biomech*, 2004. 37(9): p. 1371-7.
5. Sensinger, JW and Weir, RF, Modeling and preliminary testing socket-residual limb interface stiffness of above-elbow prostheses. *IEEE Trans Neural Syst Rehabil Eng*, 2008. 16(2): p. 184-90.
6. Andrews, J, Transhumeral and Elbow Disarticulation Anatomically Contoured Socket Considerations. *American Academy of Orthotists and Prosthetists*, 2008. 20(3): p. 5.
7. Daly, W, Upper extremity socket design options. *Phys Med Rehabil Clin N Am*, 2000. 11(3): p. 627-38.
8. Lake, C, The Evolution of Upper Limb Prosthetic Socket Design. *American Academy of Orthotists and Prosthetists*, 2008. 20(3): p. 8.
9. Lee, WC and Zhang, M, Using computational simulation to aid in the prediction of socket fit: a preliminary study. *Med Eng Phys*, 2007. 29(8): p. 923-9.
10. Anglin, C and Wyss, UP, Review of arm motion analyses. *Proc Inst Mech Eng H*, 2000. 214(5): p. 541-55.

11. Drummey, J, Enhancing the Functional Envelope: A Review of Upper-Limb Prosthetic Treatment Modalities. The Academy Today, 2009. June: p. 5.
12. Girona, RJ, Lloyd, J, Clark, ME, and Walker, RL, Preliminary evaluation of reliability and criterion validity of Actiwatch-Score. J Rehabil Res Dev, 2007. 44(2): p. 223-30.
13. Small, CF, Bryant, JT, Dwosh, IL, Griffiths, PM, Pichora, DR, et al., Validation of a 3D optoelectronic motion analysis system for the wrist joint. Clin Biomech (Bristol, Avon), 1996. 11(8): p. 481-483.
14. Lowe, B, Accuracy and validity of observational estimated of shoulder and elbow posture. Applied Ergonomics, 2004. 35: p. 13.
15. Carey, SL, Jason Highsmith, M, Maitland, ME, and Dubey, RV, Compensatory movements of transradial prosthesis users during common tasks. Clin Biomech (Bristol, Avon), 2008. 23(9): p. 1128-35.
16. Stein, RB and Walley, M, Functional comparison of upper extremity amputees using myoelectric and conventional prostheses. Arch Phys Med Rehabil, 1983. 64(6): p. 243-8.
17. Weekes, DL, Wallace, SA, and Anderson, DI, Training with an upper-limb prosthetic simulator to enhance transfer of skills across limbs. Arch. Phys. Med. Rehabilitation, 2003. 84(3): p. 7.
18. Highsmith, MJ, Carey, SL, Koelsch, KW, Lusk, CP, and Kinematic evaluation of terminal devices for kayaking with upper extremity amputation. Journal of Prosthetics and Orthotics, 2007. 19(84): p. 7.
19. Craig, JJ, Introduction to Robotics Mechanics and Control Third ed. 2005, Upper Saddle River: Pearson Education, Inc.

APPENDICES

Appendix A : Marker File

!MKR#2

[Autolabel]

C7	Cervical level 7
T10	Thoracic level 10
CLAV	Clavicle
STRN	Sternum
RBAK	Right back asymmetrical marker
RSHO	Right shoulder
WrstM	Wrist thumb side
WrstL	Wrist pinkie side
UPA	Upper arm
ELBM	
ELBL	
LSHO	Left shoulder
MWComp	Medial
LWComp	Left wrist pinkie side
ECompL	Lateral point on elbow component
ECompM	Medial Point on elbow component
BRESL	Back point on res limb
FRESL	Front point on res limb
RSckt	Right (medial) point on socket
FSckt	Left (lateral) point on socket
sLSJC	simulated LSJC (for rig)
LSJC	left shoulder joint center

CLAV,STRN,C7,T10,RBAK
BRESL,FRESL,LSHO
RSckt,FSckt,ECompL,ECompM
RSHO,RUPA,RELB
LWComp,MWComp,ECompL,ECompM
ElbM,RWRA,RWRB
Torso = C7,T10,CLAV,STRN,RBAK
LShoulder = LSHO,CLAV,T1

Appendix A (Continued)

ResLimb = BRESL,FRESL,sLSJC
Socket = RSckt,FSckt,ECompL,ECompM
LForearm = LWRA,LWRB,ECompL,ECompM
RShoulder = RSHO,CLAV,T10
RUpperarm = RSHO,RUPA,RELB
RForearm = RELB,RWRA,RWRB

Torso,RShoulder
Torso,LShoulder
RShoulder,RUpperarm
RUpperarm,RForearm
LShoulder,ResLimb
Socket,LForearm

[Segment Axes]

ORIGINTorso
AXISXTorso
AXISYTorso
AXISZTorso
ORIGINTorso,AXISXTorso
ORIGINTorso,AXISYTorso
ORIGINTorso,AXISZTorso

ORIGINRUpperarm
AXISXRUpperarm
AXISYRUpperarm
AXISZRUpperarm
ORIGINRUpperarm,AXISXRUpperarm
ORIGINRUpperarm,AXISYRUpperarm
ORIGINRUpperarm,AXISZRUpperarm

ORIGINResLimb
AXISXResLimb
AXISYResLimb
AXISZResLimb
ORIGINResLimb,AXISXResLimb
ORIGINResLimb,AXISYResLimb
ORIGINResLimb,AXISZResLimb

Appendix A (Continued)

ORIGINSocket
AXISXSocket
AXISYSocket
AXISZSocket
ORIGINSocket,AXISXSocket
ORIGINSocket,AXISYSocket
ORIGINSocket,AXISZSocket

ORIGINRForearm
AXISXRForearm
AXISYRForearm
AXISZRForearm
ORIGINRForearm,AXISXRForearm
ORIGINRForearm,AXISYRForearm
ORIGINRForearm,AXISZRForearm

ORIGINLForearm
AXISXLForearm
AXISYLForearm
AXISZLForearm
ORIGINLForearm,AXISXLForearm
ORIGINLForearm,AXISYLForearm
ORIGINLForearm,AXISZLForearm

ORIGINRWrist
AXISXRWrist
AXISYRWrist
AXISZRWrist
ORIGINRWrist,AXISXRWrist
ORIGINRWrist,AXISYRWrist
ORIGINRWrist,AXISZRWrist

ORIGINLWrist
AXISXLWrist
AXISYLWrist
AXISZLWrist
ORIGINLWrist,AXISXLWrist
ORIGINLWrist,AXISYLWrist
ORIGINLWrist,AXISZLWrist
ORIGINGlobal
AXISXGlobalAXISY
GlobalAXISZGlobal

Appendix A (Continued)

ORIGINGlobal,AXISXGlobal
ORIGINGlobal,AXISYGlobal
ORIGINGlobal,AXISZGlobal

[Joint centers]

RSJC
LSJC
REJC
ECompC
ScktC
ResLC
WrstJC
WCompJC

[Angles]

LShoulderAngles
ResLScktAngles
ElbowCompAngles
RShoulderAngles
ElbowAngles

[Distances]

DistResLSocket

Appendix B : Vicon BodyBuilder Program for Rig

Note: new part highlighted.

```
{*-----*}
{*      Biomechanical Model Of Transhumeral Prosthesis      *}
{*              Rebekah Freilich 2009              *}
{*      Master Thesis for Biomedical Engineering      *}
{*              University of South Florida              *}
{*-----*}
```

```
{*-----*}
{*Start of Macro Section*}
{*-----*}
```

```
{*Display of Segment Axis*}
{*-----*}
```

```
Macro AXISVISUALISATION(Segment)
ORIGIN#Segment=O(Segment)
AXISX#Segment={100,0,0}*Segment
AXISY#Segment={0,100,0}*Segment
AXISZ#Segment={0,0,100}*Segment
output(ORIGIN#Segment,AXISX#Segment,AXISY#Segment,AXISZ#Segment)
ENDMACRO
```

```
{*-----*}
{*End of Macro Section*}
{*-----*}
```

```
{*Define Global Origin*}
{*-----*}
```

```
Gorigin = {0,0,0}
Global = [Gorigin,{1,0,0},{0,0,1},xyz]
```

```
{*-----*}
```

Appendix B (Continued)

```
{*Definition of Virtual Points*}
{*-----*}

{*Torso*}
{*----*}

{*
BTorso= (C7+T10)/2
LTorso = (T10+STRN)/2
FTorso = (CLAV+STRN)/2
UTorso = (C7+CLAV)/2
*}

{*Shoulder*}
{*-----*}
{*
{*Temporary local coordinate system*}
TempRClav = [RSHO,C7-RSHO,1(Torso),zyx]
TempLClav = [LSHO,C7-LSHO,1(Torso),zyx]

{*
If $Static == 1 Then
    RSJC = RSHO+{0,0,-$RShoulderDepth}*Attitude(Torso)
    LSJC = LSHO+{0,0,-$LShoulderDepth}*Attitude(Torso)
    $%RSJC = RSJC/TempRClav
    $%LSJC = LSJC/TempLClav
    PARAM($%RSJC)
    PARAM($%LSJC)
EndIf
*}

{*From local coordinate system to global*}
RSJC = $%RSJC*TempRClav
LSJC = $%LSJC*TempLClav
*}

{*Elbow Component*}
{*-----*}

ECompC = (ECompL+ECompM)/2
```

Appendix B (Continued)

{*Wrist*}
{*-----*}

{*RWJC=(RWRA+RWRB)/2*}

LWJC = (LWRA+LWRB)/2

{*Residual Limb*}
{*-----*}

ResLC = (BResL+FResL)/2

{*Prosthetic Socket*}
{*-----*}

ScktC = (BSckt+FSckt)/2

{*-----*}
{*Definition of Segments*}
{*-----*}

{*
Torso = [UTorso,UTorso-LTorso,BTorso-UTorso,zyx]
*}

ResLimb = [ResLC,sLSJC-ResLC,BResL-FResL,zyx]

Socket = [ECompC,ScktC-ECompC,ECompC-LWJC,zyx]

{*RUpperm = [REJC,RSJC-REJC,REJC-RWJC,zyx]
RForearm = [RWJC,REJC-RWJC,REJC-RSJC,zxy]*}

LForearm = [LWJC,ECompC-LWJC,ECompC-sLSJC,zxy]

{*RWrist = [RWJC,REJC-RWJC,RWRA-RWRB,zxy]*}
LWrist = [LWJC,ECompC-LWJC,LWRA-LWRB,zxy]

Appendix B (Continued)

```
{*-----*}  
{*Angles*}  
{*-----*}
```

```
{*TorsoAngles = -<Global,Torso,xyz> *}
```

```
{*LShoulderAngles = <Torso,ResLimb,yxz>(-2)  
RShoulderAngles = <Torso,RUpperarm,yxz> *}
```

```
ResLScktAngles = <ResLimb,Socket,yxz>
```

```
ElbowCompAngles = <Socket,LForearm,yxz>  
{*RElbowAngles = <RUpperarm,RForearm,yxz> *}
```

```
{*-----*}  
{*Distances*}  
{*-----*}
```

```
DistResLSocket = DIST(ECompL,FResL)
```

```
{*-----*}  
{*Output*}  
{*-----*}
```

```
{*Joint Centers*}  
OUTPUT (ECompC,ScktC,ResLC,LWJC)
```

```
{*Angles*}  
OUTPUT (ElbowCompAngles)  
OUTPUT (ResFScktAngles)
```

```
{*Distances*}  
OUTPUT (DistResLSocket)
```


Appendix B (Continued)

```
{*DISPLAY*}  
{*This calls up the macro to display the segments*}  
AXISVISUALISATION(Socket)  
AXISVISUALISATION(ResLimb)  
AXISVISUALISATION(LForearm)  
AXISVISUALISATION(LWrist)  
AXISVISUALISATION(Global)
```

Appendix C: Vicon BodyBuilder Program

Note: new part highlighted.

```
{*-----*}
{*      Biomechanical Model Of Transhumeral Prosthesis      *}
{*              Rebekah Freilich 2009              *}
{*      Master Thesis for Biomedical Engineering      *}
{*              University of South Florida              *}
{*-----*}
```

```
{*-----*}
{*Start of Macro Section*}
{*-----*}
```

```
{*Display of Segment Axis*}
{*-----*}
```

```
Macro AXISVISUALISATION(Segment)
ORIGIN#Segment=O(Segment)
AXISX#Segment={100,0,0}*Segment
AXISY#Segment={0,100,0}*Segment
AXISZ#Segment={0,0,100}*Segment
output(ORIGIN#Segment,AXISX#Segment,AXISY#Segment,AXISZ#Segment)
ENDMACRO
```

```
{*-----*}
{*End of Macro Section*}
{*-----*}
```

```
{*Define Global Origin*}
{*-----*}
```

```
Gorigin = {0,0,0}
Global = [Gorigin,{1,0,0},{0,0,1},xyz]
```

Appendix C (Continued)

```
{*-----*}  
{*Definition of Virtual Points*}
```

```
{*-----*}
```

```
{*Torso*}  
{*-----*}
```

```
BTorso= (C7+T10)/2  
LTorso = (T10+STRN)/2  
FTorso = (CLAV+STRN)/2  
UTorso = (C7+CLAV)/2  
Torso = [UTorso,UTorso-LTorso,BTorso-UTorso,zyx]
```

```
{*Shoulder*}  
{*-----*}
```

```
{*Temporary local coordinate system*}  
{*TempRClav = [RSHO,C7-RSHO,1(Torso),zyx]*}  
TempLClav = [LSHO,C7-LSHO,1(Torso),zyx]
```

```
IF Static==1 Then  
    {*RSJC = RSHO+{0,0,-$RShoulderDepth}*Attitude(Torso)*}  
    LSJC = LSHO+{0,0,-$LShoulderDepth}*Attitude(Torso)  
    {*$%RSJC = RSJC/TempRClav*}  
    $%LSJC = LSJC/TempLClav  
    {*PARAM($%RSJC)*}  
    PARAM($%LSJC)  
End
```

```
{*From local coordinate system to global*}  
{*RSJC = $%RSJC*TempRClav*}  
LSJC = $%LSJC*TempLClav
```

Appendix C (Continued)

{*Elbow Component*}
{*-----*}

$$ECompC = (ECompL+ECompM)/2$$

{*Wrist*}
{*-----*}

$$\{*RWJC=(RWRA+RWRB)/2*\}$$

$$LWJC = (LWRA+LWRB)/2$$

{*Residual Limb*}
{*-----*}

$$ResLC = (RResL+LResL)/2$$

{*Prosthetic Socket*}
{*-----*}

$$ScktC = (RSckt+LSckt)/2$$

{*-----*}
{*Definition of Segments*}
{*-----*}

$$Torso = [UTorso,UTorso-LTorso,BTorso-UTorso,zyx]$$

$$ResLimb = [ResLC,LSJC-ResLC,RResL-LResL,zyx]$$

$$Socket = [ECompC,ScktC-ECompC,ECompC-LWJC,zyx]$$

$$\begin{aligned} &\{*RUpperm = [REJC,RSJC-REJC,REJC-RWJC,zyx] \\ &RForearm = [RWJC,REJC-RWJC,REJC-RSJC,zyx]*\} \\ &LForearm = [LWJC,ECompC-LWJC,ECompC-LSJC,zyx] \end{aligned}$$

Appendix C (Continued)

```
{*RWrist = [RWJC,REJC-RWJC,RWRA-RWRB,zxy]*}  
LWrist = [LWJC,ECompC-LWJC,LWRA-LWRB,zxy]
```

```
{*-----*}  
{*Angles*}  
{*-----*}
```

```
TorsoAngles = -<Global,Torso,xyz>
```

```
LShoulderAngles =<Torso,ResLimb,yxz>(-2)  
{*RShoulderAngles =<Torso,RUpperarm,yxz>*}
```

```
ResLScktAngles =<ResLimb,Socket,yxz>
```

```
ElbowCompAngles =<Socket,LForearm,yxz>
```

```
{*RElbowAngles =<RUpperarm,RForearm,yxz>*}
```

```
{*-----*}  
{*Distances*}  
{*-----*}
```

```
DistResLS = DIST(ECompL,LResL)
```

```
{*-----*}  
{*Output*}  
{*-----*}
```

```
{* Joint Centers*}  
OUTPUT(ECompC,ScktC,ResLC,LWJC,LSJC)
```

```
{*Angles*}  
OUTPUT(ElbowCompAngles)  
OUTPUT(ResLScktAngles)
```

Appendix C (Continued)

{*Distances*}

OUTPUT(DistResLS)

{*DISPLAY*}

{*This calls up the macro to display the segments*}

AXISVISUALISATION(Socket)

AXISVISUALISATION(ResLimb)

AXISVISUALISATION(LForearm)

AXISVISUALISATION(LWrist)

AXISVISUALISATION(Global)